ISSN 1027-5495. Functional Materials, 29, No.2 (2022), p. 237-243.
doi:https://doi.org/10.15407/fm29.02.237

Structure and antibacterial property of coordination polymer [Zn(4-[(8-hydroxy-5-quinolinyl)azo]-benzenesulfonic acid)$(H_2O)_4$]

***Yanan Luo*[1], *Pengfei Wang*[1], *Kangming Liu*[1], *Zhengyu Yang*[1], *MujiaSong*[1], *Xueling Cao*[2]**

[1]College of Pharmacy, Jilin Medical University, 5 Jilin Str., 132013 Jilin, P. R. China
[2]College of Science, Qiongtai Normal University, 571100 Hainan, P. R. China

Received February 15, 2022

Complex [Zn(4-[(8-hydroxy-5-quinolinyl)azo]-benzenesulfonic acid)$(H_2O)_4$] (**1**) was successfully synthesized by solvothermal synthesis by H_2L (H_2L=4-[(8-hydroxy-5-quinolinyl)azo]-benzenesulfonic acid) and Zn(II) ion. Complex 1exhibits a zero-dimensional (0D) structure, which is connected into three-dimensional (3D) supramolecular network by hydrogen bonding and π···π stacking interaction. In addition, the antibacterial property of complex **1** was tested. The antibacterial property of Gram-negative bacteria is slightly better than that of Gram-positive bacteria in complex **1**.

Keywords: hydrogen bonding, supramolecular structure, antibacterial property, π···π stacking interaction.

Структура та антибактеріальні властивості координаційного полімеру [Zn(4-[(8-гідрокси-5-хінолініл)азо]-бензолсульфоновакислота) $(H_2O)_4$]. *Yanan Luo, Pengfei Wang, Kangming Liu, Zhengyu Yang, Mujia Song, Xueling Cao*

Комплекс [Zn(4-[(8-гідрокси-5-хінолініл)азо]-бензолсульфоновакислота)$(H_2O)_4$] (1) був успішно синтезований сольвотермічним синтезом з H_2L (H_2L=4-[(8-гідрокси-5)-хінолініл)азо]-бензолсульфоновакислота) та іону Zn(II). Комплекс 1 демонструє нульвимірну (0D) структуру, яка повіязана в тривимірну (3D) супрамолекулярну мережу за допомогою водневого звіязку та взаємодії π···π стекінгу. Крім того, було перевірено антибактеріальну властивість комплексу 1. Антибактеріальні властивості грамнегативних бактерій дещо кращі, ніж у грампозитивних бактерій у комплексі 1.

1. Introduction

At the end of the 20th century, multifunctional materials represented by d10 metal coordination polymers have attracted extensive attention due to their novel structures and potential applications in the fields of separation, fluorescence, catalysis and antimicrobial applications [1–4]. Selecting appropriate metal center ions and organic ligands is a key step and an important factor in the construction of complex materials with excellent properties [5]. Recent studies have shown that d^{10} metal (such as Ag, Cu and Zn) and nitrogen ligands not only improve the stability of the ligand itself, but also make d10 metal complexes have good antibacterial properties and diverse structures, thus enriching the applications of d^{10} metal complexes in various fields [6–8].The research on organic ligands started very early. Quinoline ligand, as a typical chelat-

ing ligand, has attracted more and more attention, and its strong coordination ability has aroused great interest of researchers. Through continuous exploration and research, it was found that the complexes formed by Quinoline ligands are not only stable in structure, but also rich in hydrogen bonds. Hydrogen bonds can connect the complexes to form a supramolecular network structure with higher dimensional space [9, 10]. In addition, recently, it has been found that ligands containing sulfonic acid groups can not only be used as bridging ligands, but also form rich hydrogen bonds through three oxygen atoms, so the formed complexes have rich and diverse spatial structures [11]. Considering the above factors, d^{10} metal will react with ligands containing 8-hydroxyquinoline and sulfonic acid groups at the same time, and materials with rich structure and good antibacterial properties will be prepared through the self-assembly process. Compared with some existing antibacterial materials, the crystal materials of d10 metal complexes have the advantages of low toxicity, effectiveness and long-term efficacy [12–13].

In this paper, the complex$[Zn(L^{2-})(H_2O)_4]$ (**1**) was successfully synthesized with 4-[(8-hydroxy-5-quinoline)azo]-benzenesulfonic acid as the ligand. The crystal structure of complex **1** was determined by single crystal X-ray diffraction. Then, the complex **1** was characterized (such as elemental analysis, thermogravimetric analysis and powder X-ray diffraction). Finally, a coordination polymer with excellent potential in antibacterial activities was successfully synthesized, and the antibacterial property of complex **1** was investigated by using the bacteriostatic method and growth curve method.

2. Experimental

Synthesis of ligand H_2L. H_2L, 4-[(8-hydroxy-5-quinolinyl)azo]-benzenesulfonic acid, was prepared according to the literature method [14].

Synthesis of $[Zn(L^{2-})(H_2O)_4]$ (1). A mixture of $ZnNO_3$ (30 mg 0.158 mmol), H_2L (5 mg), 4,4′-bipyridine (5 mg), H_2O (2 mL), ethanol (10 mL) and dimethylamine (0.025 mL) was dissolved. Stir for 60 min at room temperature. The suspension was put into a Teflon-lined autoclave and kept under autogenous pressure at 130°C for 3 days. After slow cooling to room temperature, red flaky crystals were filtered and washed with ethanol and dried in the air, in about 39 % yield (based on Zn). Anal. calcd.

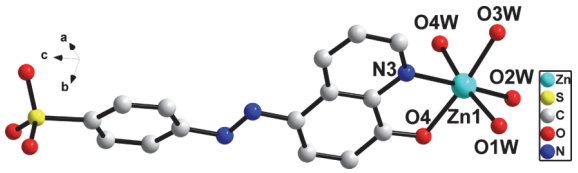

Fig. 1. The coordination environments of Zn1 in complex **1** (All hydrogen atoms are omitted for clarity).

for $C_{15}H_{17}ZnN_3O_8S$ (464.75 g/mol): C 38.76; H 3.69; N 9.06 %; found: C 38.81; H 3.61; N 9.01 %.

Structure determination. Complex **1** was stable under ambient conditions and single crystals were glued on thin glass fibers. Diffraction intensities were collected on Bruker Apex II CCD area-detector diffractometer (Mo Kα, 0.071073 nm). An empirical absorption correction was applied to the date using the SADABS program. The structure was solved by the direct method (SHELXS-97) and refined by full matrix least squares [15]. All non-hydrogen atoms were refined anisotropically. All hydrogen atoms were located geometrically by the program OLEX-2 [16]. The final formula was derived from crystallographic data combined with elemental and thermogravimetric analyses data. CCDC-930812 contains the supplementary crystallographic data for this paper.

Testing of Antibacterial property. Solution preparation for antibacterial experiment: The organic ligand (H_2L) solution with the concentration of 5 mg/mL was prepared by ultrasonic stirring of 50 mgorganic ligand in 10 mL distilled water. About 50 mg of complex **1** was stirred in 5 mL of distilled water by ultrasonically agitation to prepare a complex **1** solution with a concentration of 10 mg/mL (Solution 1). 2.5 mL of solution 1 was taken into 2.5 mL distilled water and ultrasonically stirred into a complex solution of 5 mg/mL (solution 2). Then 1.5 mL of solution 2 was taken into 1.5 mL distilled water and ultrasonically stirred into a complex solution of 2.5 mg/mL (solution 3). Filter paper treatment: Filter paper with a diameter of about 6 mm were placed into sterile distilled water, H_2L solution, solution 1, solution 2 and solution 3 respectively for ultrasound treatment. After soaking for 1 h, they were taken out and placed in a clean petri dish. Then they were placed on the aseptic operating table, irradiated for sterilization by ultraviolet lamp. Disc diffusion method was used to determine the inhibi-

Table 1. Complex **1** of crystal data collections and structure refinements

Complex **1**			
Formula	$C_{15}H_{17}ZnN_3O_8S$	Fw	464.75
Crystal system	Orthorhombic	V, nm^3	3.6089(12)
Temperature, K	296(2)	Space group	*Pcan*
α, °	90.00	ρ_{calc}, $Mg \cdot m^{-3}$	1.711
β, °	90.00	μ, mm^{-1}	1.528
γ, °	90.00	Reflections collected	3218
a, nm	0.7343(15)	*Z*	8
b, nm	1.5181(3)	*F*(000)	1904
c, nm	3.2375(6)	θ range, °	1.26?25.10
Final $R^{a,b}$ indices [$I>2\sigma(I)$]	R_1 = 0.0668	*R* indices (all data)	R_1 = 0.1521
		wR_2 = 0.1398	
Independent reflections (R_{int})	1618 (0.1769)	GOF	1.019

Table 2. Selected bond lengths (nm) and angles (°) for complex **1**

Complex **1**			
Zn1–O1W	0.2061(5)	Zn1–O2W	0.2139(5)
Zn1–O3W	0.2096(5)	Zn1–O4W	0.2102(5)
Zn1–O4	0.2082(5)	Zn1–N3	0.2134(6)
O1W–Zn1–O4	93.6(2)	O1W–Zn1–O3W	87.9(2)
O4–Zn1–O3W	171.6(2)	O1W–Zn1–O4W	168.8(2)
O4–Zn1–O4W	91.1(2)	O3W–Zn1–O4W	88.9(2)

tion zones in the growth of bacterial species. Escherichia coli (ATCC25922) and Staphylococcus aureus (ATCC6538) were selected and inoculated into sterile nutrient agar. After the nutrient agar medium was cooled and shaped, filter papers of the blank water sample, H_2L ligand, solution 1, solution 2 and solution 3 were placed in a fixed position. The culture was conducted in an incubator with a constant temperature of 37°C for 2–3 days and observed every 6 h. Gram growth curve experiment: complex **1** of different weights was dissolved in the sterilized liquid medium, sealed and stirred by ultrasound. Medium solutions containing complex **1** at concentrations of 0, 12.5, 25, 50, 100, 200 and 400 μg/mL were placed in a sterile platform for UV irradiation for sterilization. A certain amount of Escherichia coli culture was inoculated into the liquid medium with the same volume and different concentrations of complex **1**, and placed in an incubator of 37°C for shock culture. At 0, 3, 6, 9, 12, 16, 18, 21 and 24 h, the absorbance of the above solution (including the same volume of Escherichia coli and different concentrations of complex **1**) at fixed wavelength of 600 nm (according to the literature) was measured by an UV-Vis spectrophotometer [17].

3. Results and discussion

$[Zn(L^{2-})(H_2O)_4]$ (**1**) was synthesized by traditional solvothermal method with $ZnNO_3$ and H_2L. Single-crystal X-ray diffraction analysis reveals that complex **1** crystallizes in the Orthorhombic system, space group *Pcan*, which exhibits a 0D structure (Table 1). In addition, the asymmetric structural unit of complex **1** contains a Zn(II) ion, an L^{2-} ligand and four coordinated H_2O molecules (Fig. 1C).

Zn(II) ion is six coordinated by fiveoxygenatoms and a nitrogen atom. Among them, Zn1 is coordinated by O1W, O2W, O3W, O4W from four different H_2O molecules respectively, and N3, O4 from a single L^{2-} ligand molecule, forming a slightly twisted octahedral structure. In complex **1**, the L^{2-} ligand adopted chelation coordination mode. In addition, the bond symbol й range of Zn1 is [82.0(2)°–171.6(2)°]. The

Table 3. Hydrogen bond distances [nm] and angles [°] in complex **1**

D–H	d(D–H)	d(H···A)	DDHA	d(D–A)	A
O1W–H1WB	0.085	0.198	144	0.2710(7)	$O4^{i}$
O4W–H4WB	0.087	0.195	145	0.2710(7)	$O4^{ii}$
O4W–H4WA	0.087	0.195	135	0.2644(8)	$O2^{iii}$
O3W–H3WB	0.085	0.238	122	0.2929(8)	$O1^{iv}$
O2W–H2WA	0.085	0.227	163	0.3088(8)	$O3W^{v}$
O2W–H2WB	0.085	0.196	149	0.2728(8)	$O3^{vi}$

Symmetry codes for complex **1**: i, −0.5 + *x*, 0.5 − *y*, *z*; ii, 0.5 + *x*, 0.5 − *y*, *z*; iii, 1.5 − *x*, −0.5 + *y*, 1 −*z*; iv, 0.5 − *x*, −0.5 + *y*, 1 −*z*; v, *x*, −*y*, 0.5 −*z*; vi, 1 − *x*, *y*, −0.5 + *z*

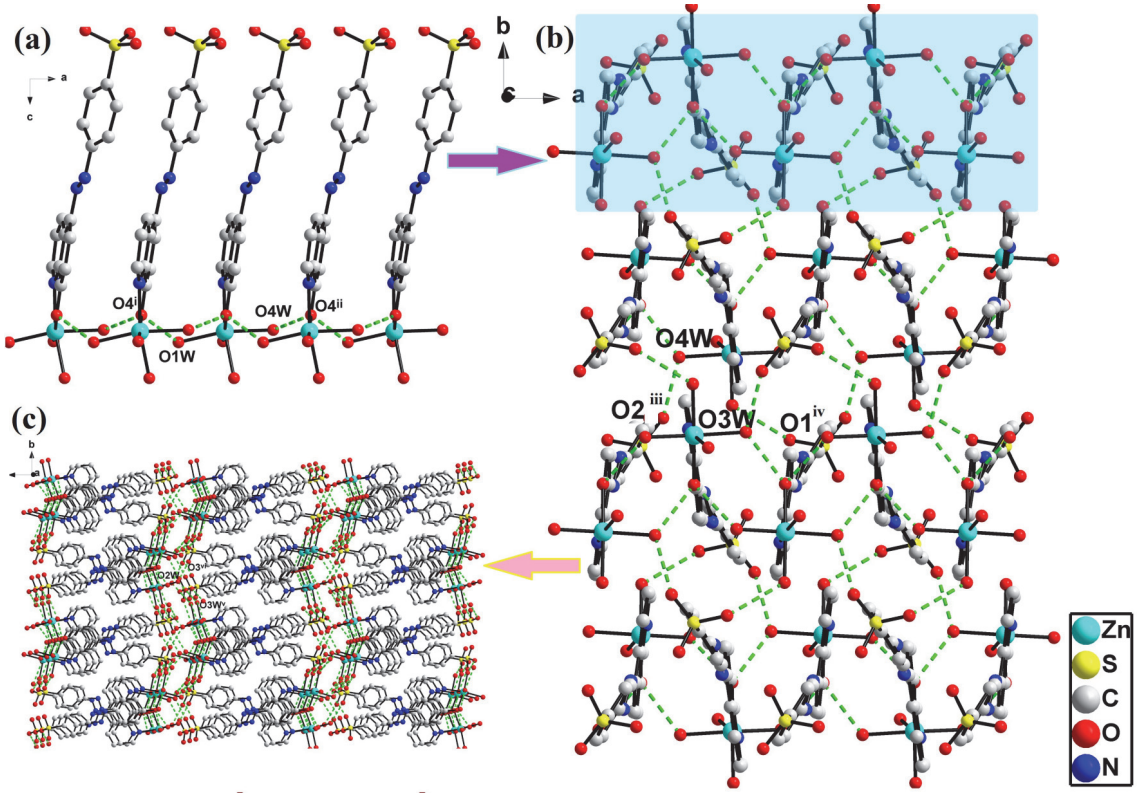

Fig. 2. (a) 1D chain structure; (b) 2D layer structure; (c) 3D supramolecular structure via hydrogen bonds interactions of complex **1** (symmetry codes: i, −0.5 + *x*, 0.5 − *y*, *z*; ii, 0.5 + *x*, 0.5 − *y*, *z*; iii, 1.5 − *x*, −0.5 + *y*, 1 −*z*; iv, 0.5 − *x*, −0.5 + *y*, 1 −*z*; v, *x*, −*y*, 0.5 −*z*; vi, 1 − *x*, *y*, −0.5 + *z*. All hydrogen atoms are omitted for clarity.

distances of Zn–O/N [0.2061(5)–0.2139(5) nm] are comparable with those found in other related Zn(II) complexes (Table 2).

In the crystal building, the 0D structure is connected into a three-dimensional supramolecular network structure by hydrogen bonding (Table 3). Along the a axis, O1W and O4W atoms in different H_2O molecules are connected with $O4^{i}$ and $O4^{ii}$ on the adjacent 8-hydroxyquinoline[d(O1WO4^{i}) = 0.2710(7) nm, ∠ O1W–H1WBO4^{i} = 144°; d(O4WO4^{ii}) = 0.2710(7) nm, ∠ O4W-H4WBO4^{ii} = 145°], forming a one-dimensional (1D) chain structure (Fig. 2a). In addition, along the *b* axis O4W and O3W atoms from H_2O molecules are connected with $O2^{iii}$ and $O1^{iv}$ on sulfonic acid groups in adjacent chains [d(O4WO2^{iii}) = 0.2644(8) nm, ∠ O4W–H4WAO2^{iii} = 135°; d(O3WO1^{iv}) = 0.2929(8) nm, ∠ O3W–H3WBO1^{iv} = 122°], forming a two-dimensional (2D) layered structure (Fig. 2b). Finally, as a hydrogen bond donor, O2W atom is connected with $O3W^{v}$ and $O3^{vi}$ in the two adjacent layers to form a 3D network

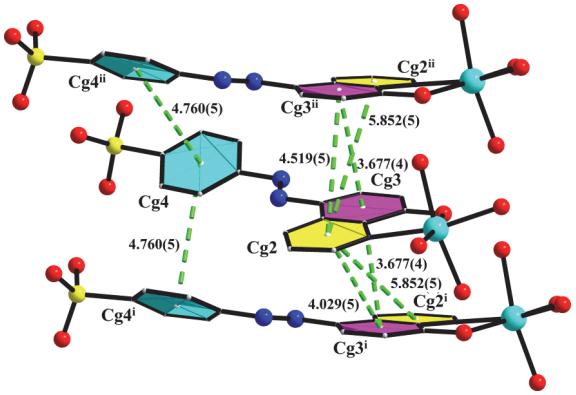

Fig. 3. 2D layer structure via π···π interactions of complex **1** (symmetry codes: i, −0.5 + *x*, 0.5 − *y*, *z*; ii, 0.5 + *x*, 0.5 − *y*, *z*. All hydrogen atoms are omitted for clarity.

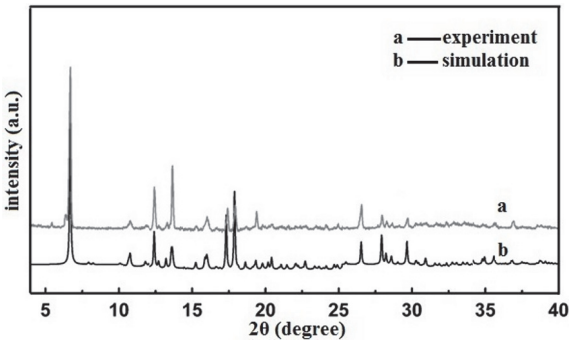

Fig. 4. The experimental (a) and simulative (b) powder X-ray diffraction patterns for complex **1**.

structure [d(O2WO3W^{v}) = 0.3088(8) nm, ∠ O2W–H2WAO3W^{v} = 163°; d(O2WO3^{vi}) = 0.2728(8) nm, ∠ O2W–H2WBO3^{vi} = 149°] (Fig. 2c). In the crystal building, due to the H_2L ligand containing 8-hydroxyquinoline and benzene rings, there are abundant π–π stacking interaction (Fig. 3). The range of center distance between 8-hydroxyquinoline and benzene rings was calculated by Platon program as [3.677(4)–5.852(5) Å], and complex **1** was connected to form 2D supramolecular layered structure (Table 4). Noncovalent bonding forces such as hydrogen bonding and π···π stacking interaction play an important role in building and stabilizing the supramolecular grid structure of complex **1**.

In order to confirm the structural homogeneity of the bulk power materials, Power X-ray diffraction (PXRD) experiment has been carried out. The PXRD experimental and computer-simulated patterns are in good agreement with each other (Fig. 4), indicating phase purity of complex **1**.

In order to further determine the thermal stability of complex **1**, thermogravimetric analyzer has been determined. The experimental results show that the weight loss from 120 to 158°C is consistent with the removal of four coordinated H_2O molecules (exp. 15.49 %, cal. 15.45 %). The total weight loss of 66.98 % from 220°C to 340°C can be attributed to the release of a

Table 4. Selected π–π interactions geometry for complex **1**

Complex **1**						
Cg(I) → Cg(J)	Cg–Cg,	α, °	β, °	γ, °	CgI_Perp,	CgJ_Perp,
Cg2 → Cg2^{i}	5.852(5)	16	43.52	59.60	2.961(3)	−4.244(3)
Cg2 → Cg2^{ii}	5.852(5)	16	59.60	43.52	−4.244(3)	2.961(3)
Cg2 → Cg3^{i}	4.029(5)	13.8(4)	25.95	39.47	3.110(3)	−3.623(3)
Cg2 → Cg3^{ii}	4.519(5)	13.8(4)	37.54	24.30	−4.118(3)	3.583(3)
Cg3 → Cg3^{i}	3.677(4)	11	12.11	8.82	3.633(3)	−3.595(3)
Cg3 → Cg3^{ii}	3.677(4)	11	8.82	12.11	−3.595(3)	3.633(3)
Cg4 → Cg4^{ii}	4.760(5)	61	11.64	70.66	−1.577(4)	4.663(4)

Cg(I) = Plane number I (= ring number in () above) (Cg2 = N3 → C1 → C2 → C3 → C4 → C5; Cg3 = C4 → C5 → C6 → C7 → C8 → C9; Cg4 = C10 → C11 → C12 → C13 → C14 → C15) (Symmetry codes for complex **1**: i, −0.5 + *x*, 0.5 − *y*, *z*; ii, 0.5 + *x*, 0.5 −*y*, *z*).
Cg–Cg = Distance between ring Centroids (Ang.)
Alpha = Dihedral Angle between Planes I and J (Deg)
Beta = Angle Cg(I) → Cg(J) or Cg(I) → Me vector and normal to plane I (Deg)
Gamma = Angle Cg(I) → Cg(J) vector and normal to plane J (Deg) CgI_Perp = Perpendicular distance of Cg(I) on ring J (Ang.)
CgJ_Perp = Perpendicular distance of Cg(J) on ring I (Ang.)

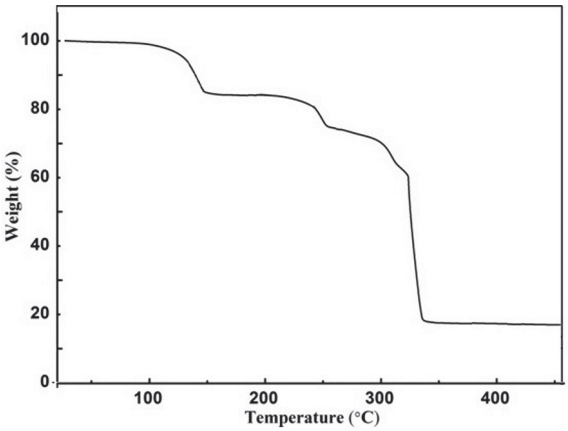

Fig. 5. TGA curve of complex **1**.

L^{2-} ligand (cal. 67.03 %). According to weight loss analysis, the final product may be ZnO? (exp. 17.48 %, cal. 17.52 %) (Fig. 5).

As shown in Fig. 6a and b, the antibacterial activities of complex **1** were studied against Gram-negative Escherichia coli (E. coli) and Gram-positive Staphylococcus aureus (S. aureus). The results showed that filter paper with blank H_2L ligand and low concentration of complex **1**had no antibacterial activity against E. coli and S. aureus in Petri dishes. Subsequently, with the increasing concentration of complex **1**, the high concentration of complex **1** showed relatively excellent antibacterial activity against both E. coli and S. aureus. In addition, in Fig. 6a and b, it can be seen that complex **1** has stronger inhibitory effect and better antibacterial performance on E. coli compared with S. aureus. By comparing the antibacterial activities of H_2L ligand and complex **1** of different concentrations, it was indicated that the ligand itself did not have antibacterial activities, and the inhibition zone of the complex **1** with the concentration of 5 mg/mL was larger than other concentrations. The results indicated that complex **1** had a good antibacterial activity, which was mainly due to the slow release of the complex **1** to Zn^{2+}.

In order to further study and verify the antibacterial activities, the effect of complex **1** on the growth of E. coli was tested. The results showed that the growth curve of E. coli treated with 12.5, 25 and 50 μg/mL complex **1** was almost the same as that treated with 0 μg/mL complex **1**, showing typical growth curve (Fig. 7). Therefore, it was shown that complex **1** had no inhibitory effect on E. coli at low mass concentration. OD600 of E. coli treated with 100, 200 and 400 μg/mL of complex **1** showed no obvious

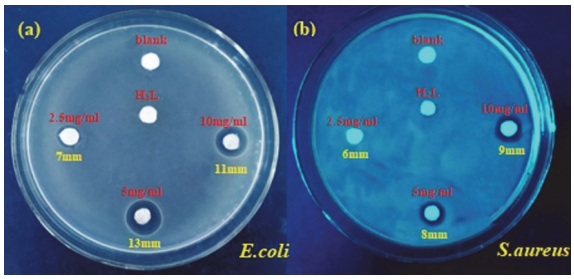

Fig. 6. (a) Optical photograph of complex **1** for negative E. coli; (b) Optical photograph of complex **1** for positive S. aureus.

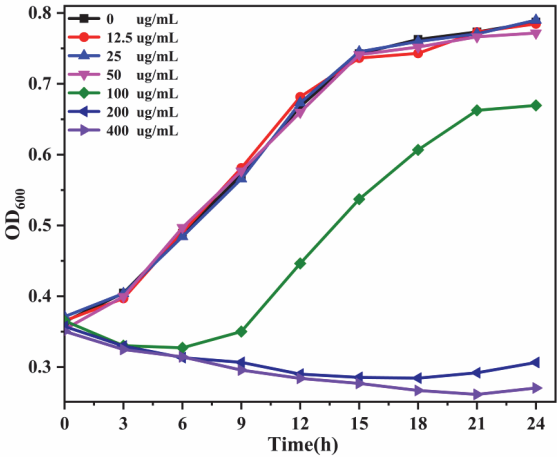

Fig. 7. Growth curves of E.coli in different concentrations of complex **1**.

change at about 6–9 h compared with OD600 atinitial stage, indicating that complex **1** had inhibitory effect on the growth of E. coli. However, with the extension of time, the growth trend of E. coli treated with 100 μg/mL complex **1** tended to the typical E. coli growth curve, which indicated that the delay period of E. coli was prolonged relative to the low concentration. After 24 h culture, the highest OD600 of E. coli treated with 100 μg/mL complex **1** was close to the control group at 0 μg/mL. That is, when E. coli reached a certain level, complex **1** with a mass concentrationless than 100 μg/mL could no longer inhibit the growth of E. coli. Only complex **1** with a mass concentration 200 μg/mL could completely inhibit the proliferation and growth of E. coli in the culture medium within 24 h.

The antibacterial activities of complex **1** mainly depend on the release of Zn^{2+}. Through the continuous release of Zn^{2+}, the original chemical balance between Zn^{2+} and ligand and the ion channel of metal ion transport is destroyed, and the integrity of cell membrane is finally destroyed, thus

achieving the purpose of antibacterial. Through the study of the antibacterial properties of complex **1**, it was found that complex **1**, as the storage of metal ions, could continuously release Zn^{2+} with the collapse of complex structure, which was the main reason forthe continuous antibacterial effect of complex **1** material. Complex **1** is an insoluble solid material, which may be a good solid antibacterial agent.

4. Conclusion

In this paper, a Zn(II)-based coordination polymer $[Zn(L^{2-})(H_2O)_4]$ with 0D structure was successfully synthesizedby solvothermal synthesisusing H_2L ligand and Zn(II) ion. The 0D structure is connected into a 3D supramolecular network structure by hydrogen bonding and π···π stacking interaction. Complex **1** showed good antibacterial properties in the inhibitory region of Gram-negative E. coli. And complex **1** with a mass concentration of more than 200 μg/mL could completely inhibit the proliferation and growth of E. coli in the culture medium within 24 h. It also indicated that the crystal material of the complex **1** had a good application potential in the field of biology.

Acknowledgment

This work was supported by the National Science Foundation of China (grant No. 21902058), Natural Science Foundation of Jilin Province (20180101191JC), the major project in Jilin institute of chemical technology (No.2018021)?the project in Jilin Medical University (No. JYBS2021019LK)?Project of Science and Technology Development of Jilin City (No.20190104161), the science and technology project in Jilin Province Departmentaof Education (No. JJKH20220458KJ).

References

1. B.Parmar, K.K.Bisht, Y.Rachuri et al., *Inorg.Chem.Front.*, **7**, 10821107 (2020).
2. S.Chand, A.Pal, R.Saha et al., *Inorg.Chem.*, **59**, 70567066 (2020).
3. A.Golmohamadpour, B.Bahramian, M.Khoobi et al., *Photodiagn.Photodyn.*, **23**, 331338 (2018).
4. J.Wang, L.Zhou, C.Rao et al., *Dyes and Pigments*, **190**, 109285 (2021).
5. D.C.Hu, Y.Fan, C.D.Si et al., *J.Solid State Chem.*, **241**, 198204 (2016).
6. M.Nakhaei, K.Akhbari, M.Kalati et al., *Inorg. Chem.Acta*, **522**, 120353 (2021).
7. S.Bouson, A.Krittayavathananon, N.Phattharasupakun et al., *R.Soc.Open Sci.*, **4**, 170654 (2017).
8. M.Hajibabaei, R.Zendehdel, Z.Panjali, *J. Inorg.Organomet.P.*, **30**, 46224626 (2020).
9. K.Takahashi, T.Sato, H.Mori et al., *Hyperfine Interact.*, **206**, 15 (2012).
10. Y.S.Shi, Q.Yu, J.W.Zhang et al., *CrystEngCommv*, **23**, 16041615 (2021).
11. Y.N.Luo, H.Y.Jiang, L.Y.Yu et al., *Inorg. Chem.Commun.*, **86**, 304307 (2017).
12. M.Can, S.Demirci, A.K.Sunol et al., *Micropor. Mesopor.Mat.*, **309**, 110533 (2020).
13. B.P.Xie, J.W.Chai, C.Fan et al., *ACS Appl. Bio Mater.*, **3**, 85258531 (2020).
14. J.S.Park, S.Jeong, S.Dho et al., *Dyes & Pigments*, **87**, 4954 (2010).
15. O.V.Dolomanov, L.J.Bourhis, R.J.Gildea et al., *J.Appl.Crystallogr.*, **42**, 339 (2009).
16. G.M.Sheldrick, SHELXTL NT Crystal Structure Analysis Package[CP]. Version 5.10; Bruker AXS, Analytical X-ray System: Madison, WI (1999).
17. X.J.Duan, X.D.Du, B.B.Zhang et al., *Biomedical Engineering and Clinical Medicine*, **19**, 237 (2015).